INTERNATIONAL JOURNAL of PARTICLE THERAPY

Does Neutron Radiation Therapy Potentiate an Immune Response to Merkel Cell Carcinoma?

Stephanie K. Schaub, MD[1]; Robert D. Stewart, PhD[1]; George A. Sandison, PhD[1]; Thomas Arbuckle, CMD[1]; Jay J. Liao, MD[1]; George E. Laramore, PhD, MD[1]; Jing Zeng, MD[1]; Ramesh Rengan, MD, PhD[1]; Yolanda D. Tseng, MD[1]; Nina A. Mayr, MD[1]; Shailender Bhatia, MD[2]; Paul T. Nghiem, MD, PhD[3]; Upendra Parvathaneni, MBBS, FRANZCR[1]

[1]Department of Radiation Oncology, University of Washington School of Medicine, Seattle, WA, USA
[2] Division of Medical Oncology, Department of Medicine, University of Washington School of Medicine, Seattle, WA, USA
[3] Department of Dermatology, University of Washington School of Medicine, Seattle, WA, USA

Abstract

Background: Merkel cell carcinoma (MCC) is a rare and aggressive cutaneous malignancy. In the advanced setting, MCC is often treated with immune checkpoint inhibitors such as anti-PD-1/PD-L1 antibodies. X-ray radiation therapy (XRT) is commonly used for palliation. There is an unmet need for new treatment options in patients progressing on immunotherapy and XRT. We present 2 patients with progressive MCC who were successfully treated with high linear energy transfer neutron radiation therapy (NRT).

Clinical Observations: Patient A, an 85-year-old white male with chronic lymphocytic leukemia had progressive MCC with multiple tumors on the face despite prior XRT and ongoing treatment with pembrolizumab. The 5 most symptomatic lesions were treated with a short course of NRT (2×3 Gy) while continuing pembrolizumab. All irradiated facial lesions demonstrated a complete response 2 weeks after NRT. Remarkably, an additional 4 lesions located outside the NRT fields also completely resolved. Patient B, a 78-year-old white male with no immunosuppressive condition had recurrent MCC in the scalp and bilateral cervical nodes. The painful, ulcerative tumors on his scalp were progressing despite multiple courses of XRT and multiple immunotherapy regimens, including pembrolizumab. He was treated with NRT (16-18 Gy) to the scalp and had a complete response with successful palliation. While his disease subsequently progressed outside the NRT fields, the response to NRT bridged him to receive further investigational immunotherapies, and he remains disease free 3 years later.

Conclusion: Short courses of high linear energy transfer particle therapy deserve consideration as a promising modality for local tumor control in XRT refractory tumors. The out-of-field response suggests that NRT has potential for synergizing with immunotherapy. While more data are required to identify optimal NRT parameters, the NRT dose that potentiates an antitumor immune response appears to be well below organ-at-risk tolerance.

Keywords: neutron radiotherapy; high LET radiation; Merkel cell carcinoma; MCC; immunotherapy; abscopal effects

Submitted 13 Mar 2018
Accepted 13 Jun 2018
Published 21 Sep 2018

Corresponding Author:
Upendra Parvathaneni
Department of Radiation Oncology
University of Washington,
Seattle, WA 98195, USA
Phone: + (206) 598-4101
upendra@uw.edu

Report

DOI
10.14338/IJPT-18-00012.1

http://theijpt.org

Introduction

Merkel cell carcinoma (MCC) is a rare and aggressive cutaneous malignancy that is typically sensitive to conventional x-ray radiation therapy (XRT) and has a disease-specific mortality of approximately 40% [1]. Responses to chemotherapy are not durable with a median progression-free survival of 3 months [2]. Approximately 50% of patients respond to immune checkpoint blockade in the advanced or metastatic stages, with a complete response observed in 15% [3]. There is an unmet need for novel treatment options for patients with tumors that are refractory to immunotherapy and XRT.

Fast neutron radiation therapy (NRT) is a form of high linear energy transfer (LET) radiation with a relative biological effectiveness (RBE) similar to therapeutic carbon ions. In comparison, XRT is a low LET form of radiation. Use of NRT is advantageous for the treatment of selected radioresistant tumors, such as salivary gland tumors [4, 5]. The attractiveness of NRT is largely driven by the ability of high LET radiation to overcome mechanisms of tumor radioresistance to low LET radiation, including increased survival of tumor cells irradiated in a hypoxic environment [6], cell cycle effects [7–10], cell proliferation [11], and differential repair of complex forms of DNA damage induced by low and high LET radiations [12, 13]. Cells irradiated by high LET radiations tend to accumulate in the G2/M phase of cell cycle for long periods of time and undergo mitotic catastrophe more frequently than cells irradiated by low LET radiations. Inflammatory cell death modes, such as mitotic catastrophe and necroptosis, are important initiating events to stimulate antitumor immunity [14–16], and high LET radiations may be an attractive modality for stimulating out-of-field immunogenic effects in tumors refractory to low LET radiations.

In this work, we present a new case study (patient A) that highlights the effectiveness of a short course of NRT for the treatment of MCC that was previously refractory to low LET radiation. The patient was progressing on anti-PD1 immunotherapy approximately 1 month before NRT. In this immune-suppressed patient, NRT produced a complete response within the treatment field while also triggering a putative immune-mediated, out-of-field clinical response. The term "abscopal effect" is used to describe the phenomenon when localized radiation therapy is associated with regression of metastatic lesion(s) located outside the radiation field(s) by a putative immune-mediated mechanism [17]. The exact underlying mechanism(s) and triggers to reproducibly generate this effect remain to be elucidated. To gain insight into the clinical significance of short-course NRT as it relates to in-field and out-of-field organ at risk (OAR) toxicity, updated dosimetry and clinical observations for a previously reported patient case by Macomber et al [18] is also presented (patient B). This case series illustrates the use of NRT in combination with immunotherapy to achieve potentially durable clinical responses in patients who had exhausted other treatment options. Prospective clinical trials are needed to identify optimal treatment parameters in combined radiation and immunotherapy treatments.

Fast Neutron RBE, OAR Constraints, and Treatment Planning

The University of Washington clinical neutron therapy system (CNTS) generates fast neutrons by directing 50.5 MeV protons at a beryllium target. Fast neutrons (15-30 MeV average energy) subsequently pass through a primary collimator, flattening filter, and secondary collimator with 40 individually movable leaves. The CNTS neutron beam has depth dose and lateral profiles similar to those produced by a 6 MV x-ray medical linear accelerator. For a typical NRT fraction size of 1.15 Gy per day, and using megavoltage XRT as the standard radiation for comparison, the clinical RBE for CNTS neutrons are ~3 to 4 for most OARs and up to 8 for some tumors [19, 20]. Both of the patients were treated with 3-dimensional conformal radiation therapy planning techniques using a neutron-specific beam model in the Pinnacle treatment planning system [21]. **Table 1** lists OAR plan constraints for n = 16 fractions (conventional NRT), n = 10 fractions, and n = 2 fractions (short-course NRT). Additional details of the models and methods used to estimate neutron RBE and the equivalent dose in 2 Gy fractions (EQD2) are detailed in the **Appendix**. For hypofractionated NRT, the neutron RBE ranges from 2.9 (skin, end point = telangiectasia) to 3.9 (lens, end point = cataracts). The RBE values reported in **Table 1** are based on using the same number of fractions for the XRT and NRT treatments (ie, n = 2, 10, and 16). When the NRT treatment is compared with conventionally fractionated XRT, the neutron RBE ranges from 3.5 to 5.0 (n = 16 fractions of NRT) to 5.6 to 9.7 (n = 2 fractions of NRT).

Patient A: Progression on Anti-PD1 Immunotherapy and Treated with a Short-Course of NRT

Patient A was an 85-year-old white male with a history of chronic lymphocytic leukemia (previously treated with rituximab) and recurrent MCC involving multiple skin and subcutaneous lesions on the face and scalp. The patient was initially diagnosed with

Table 1. Comparison of XRT and NRT OAR plan constraints for n = 2, 10, and 16 fractions. Neutron RBE is computed as the ratio of the XRT to NRT dose for the same number of fractions.[a]

		Megavoltage x-ray constraints (Gy)					NRT constraints (Gy)			RBE		
OAR for planning	Clinical endpoint	EQD2	α/β (Gy)	(n = 2)	(n = 10)	(n = 16)	(n = 2)	(n = 10)	(n = 16)	(n = 2)	(n = 10)	(n = 16)
Optic nerve	Blindness	50.0	2.4	18.6	36.3	43.1	6.0	9.9	11.0	3.1	3.7	3.9
Optic chiasm	Blindness	50.0	2.4	18.6	36.3	43.1	6.0	9.9	11.0	3.1	3.7	3.9
Retina	Blindness	45.0	3.8	19.3	35.5	41.0	6.3	10.0	11.0	3.1	3.5	3.7
Lens	Cataract	10.0	1.0	6.8	13.0	15.3	1.7	2.3	2.5	3.9	5.6	6.2
Ear	Acute serous otitis	30.0	4.4	15.7	27.0	30.5	5.0	7.4	8.0	3.1	3.6	3.8
Ear	Chronic serous otitis	45.0	4.4	20.0	36.0	41.3	6.5	10.3	11.3	3.1	3.5	3.6
Skin	Telangiectasia	50.0	10.0	26.1	42.2	46.5	8.9	13.3	14.3	2.9	3.2	3.2
Lacrimal gland	Dry eye	40.0	0.9	14.3	29.8	36.5	4.3	7.2	8.0	3.3	4.1	4.6
Brain	Necrosis infarction	60.0	1.7	19.4	39.3	47.5	6.2	10.7	12.0	3.1	3.7	4.0
Brainstem	Necrosis infarction	60.0	1.7	19.4	39.3	47.5	6.2	10.7	12.0	3.1	3.7	4.0

Abbreviations: RBE, relative biological effectiveness; NRT, neutron radiation therapy; XRT, x-ray therapy; OAR, organ at risk; EQD2; equivalent dose at 2 Gy.

[a]To compute the neutron RBE relative to XRT for conventional fractionation, divide the value of EQD2 by the neutron dose (n = 2, 10 and 16 fractions).

MCC of the glabellar region, for which he underwent wide-local excision with positive margins, and lymphovascular invasion. On sentinel lymph node biopsy, he had an involved right level-2 lymph node. Initial stage was pT2N1aM0 (stage IIIA). Although tumor immunohistochemistry for MCPyV was positive, serology for Merkel cell polyomavirus (MCPyV) oncoprotein antibodies was negative before his resection. Because of multiple medical comorbidities and his inability to attend a 4.5- to 5-week course of conventionally fractionated XRT (~2 Gy per day), a single-fraction radiation therapy (1 × 8 Gy) was delivered postoperatively to the primary surgical bed and the involved neck level using a mix of electrons and megavoltage x-rays. Eleven weeks later, he developed 2 out-of-field dermal recurrences on his right eyelid and premaxilla, which were treated with 8 and 10 MeV (low LET) electrons using 1 × 8 Gy.

After an initial response, the patient exhibited in-field progression within 6 weeks and further developed 3 additional dermal lesions. Anti-PD1 immunotherapy with pembrolizumab was initiated 2 months after the recurrences were detected. However, the patient's facial lesions continued to progress, and new dermal and subcutaneous lesions developed diffusely over his face and scalp (**Figure 1A** and **1B**). The originally treated postoperative sites of potential microscopic disease at glabella and level-2 lymph nodes did not recur. The patient continued on anti-PD1 immunotherapy and was referred for palliative radiation therapy to the sites of symptomatic progression.

Another month later, NRT was delivered to 3 of the most symptomatic recurrent lesions: (1) the left premaxilla, 24 × 18 mm^2; (2) left eyebrow/lid, 18 × 14 mm^2; (3) right premaxilla, 25 × 25 mm^2. The gross tumors received a total of 6 Gy in 2 fractions separated by a week (3 Gy per fraction) using 3-dimensional conformal planning (**Figure 1A** and **1B**; **Figures 2A** through **2D**). After a rapid response, 2 additional symptomatic lesions: (1) right eyelid, 25 × 14 mm^2; (2) right forehead, 15 × 8 mm^2, were similarly treated to a total NRT dose of 6 Gy (3 Gy per fraction). Four measurable nonoverlapping asymptomatic index lesions remained untreated: (1) left preauricular; 25 × 27 mm^2; (2) right preauricular, 25 × 17 mm^2; (3) left temple, 28 × 25 mm^2; and (4) left forehead, 14 × 15 mm^2. Index lesions 1 and 2 were abutting the NRT field edge (50% isodose) (**Figure 3**), while lesions 3 and 4 were unrelated to any of the NRT fields.

Within 2 weeks, all NRT-treated lesions achieved a complete clinical response (**Figure 1C** and **D**; **Figure 2E** through **H**). In addition, the 4 out-of-field index lesions exhibited a complete clinical response (**Figure 1C** and **D**; **Figure 2E** through **H**). The patient had transient grade 1 dermatitis (Common Terminology Criteria for Adverse Events [CTCAE] version 4) within the NRT field, which resolved within 1 week. There were no immunotherapy-related adverse events. Four-months after radiation, 1 of the 4 out-of-field lesions (index lesion No. 4 in **Figure 2** on the left forehead) was biopsy positive for MCC, although the patient remained asymptomatic. His serology was repeated just before the biopsy. While he had a negative MCPyV T-oncoprotein serology at the time of his initial diagnosis, this titer was found to be increased significantly 4 months after completing NRT. The seroconversion could possibly represent a new humoral immune response against the MCPyV facilitated by NRT plus pembrolizumab versus being related to increased tumor burden (ie, increased overall expression of T antigen, which is known to correlate with the antibody titers). Efforts are underway to explore the interpretation of this finding. Nine months later, the patient remains clinically and radiologically without any evidence of disease. The patient continues on pembrolizumab.

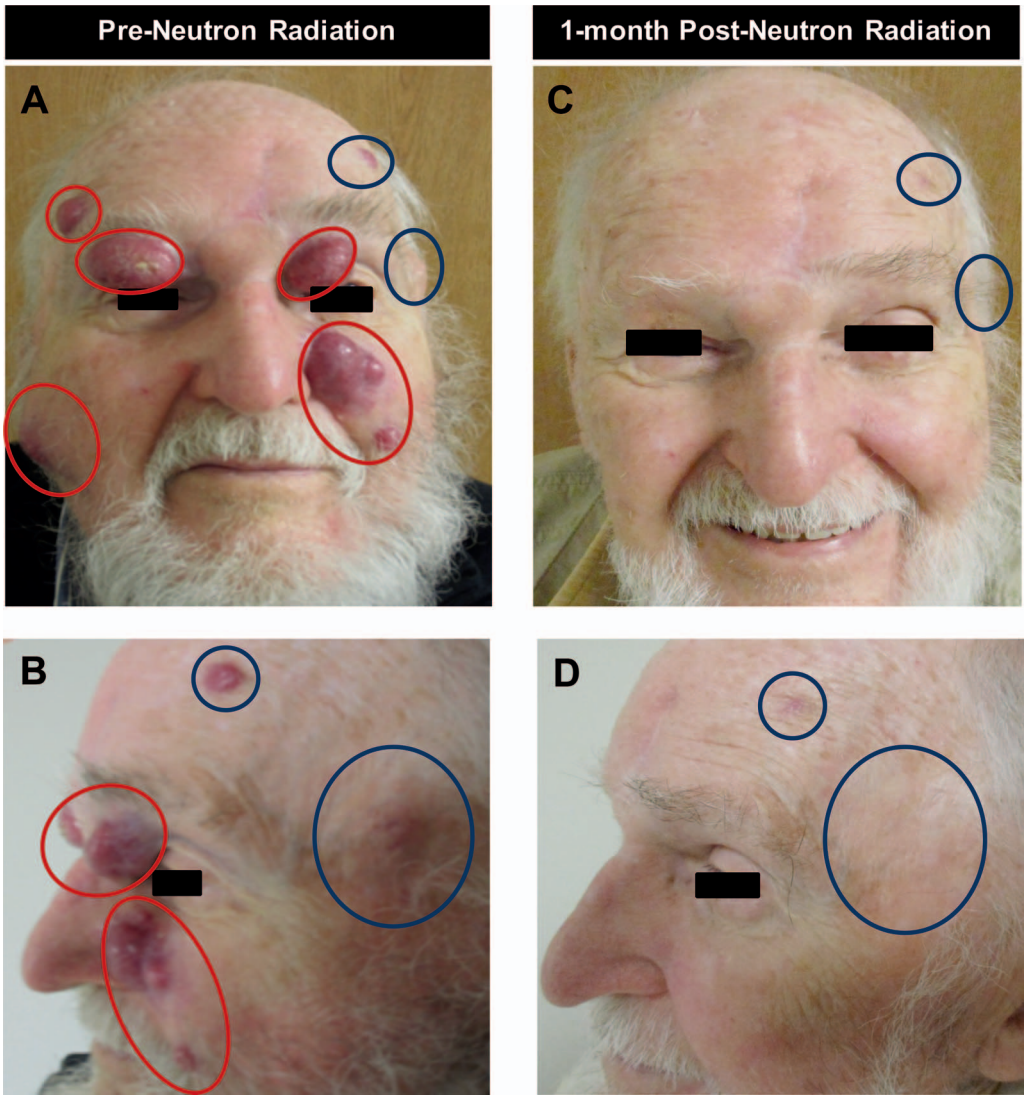

Figure 1. Patient A before and after neutron radiation treatment response of in-field (red circles) and out-of-field (blue circles) lesions. Lesions in red were targeted with 2 fractions of 3 neutron-Gy, delivered weekly (panels A and B). Complete response observed within and out of the neutron treatment fields 1 month after radiation therapy (panels C and D).

Patient B: Update on Patient with Progression on Anti-PD1 Immunotherapy and Treated with NRT

As reported in Macomber et al [18], a 78-year-old white male with no history of immunosuppression had recurrent MCC disease following intralesional and systemic anti-PD1 immunotherapy (pembrolizumab) with disease progression inside and outside prior low LET radiation therapy fields. The patient was treated with definitive doses of fractionated NRT for the fungating gross disease on the central scalp to a total dose of 18 Gy neutron in 12 fractions (1.5 Gy per day, 4 days per week), the bilateral parotid/cervical lymph nodal disease (18 Gy neutron in 10 fractions), and frontal scalp lesions (16 Gy neutrons in 8 fractions). All known sites of disease were treated, and the patient had a complete clinical and radiologic response.

Six months after NRT, he developed 3 small scalp recurrences outside the high-dose NRT fields. At that point, he was treated with monthly injections of long-acting octreotide, but his disease continued to progress with growth of these lesions. In March 2016, he subsequently enrolled in an investigational immunotherapy trial and at week 24 exhibited a radiologic complete response. However, treatment was eventually discontinued due to presence of microscopic residual MCC cells at a biopsied scalp lesion. At this time, he was restarted on anti-PD1 systemic therapy with pembrolizumab. Three years after treatment, the patient is doing well continuing pembrolizumab with no signs of MCC recurrence.

Importantly, his disease has never recurred within the high-dose NRT field, and the palliative response to NRT bridged him to receive therapy in a subsequent investigational trial. Patient B developed CTCAE v4 grade 2 xerostomia (dry mouth) and decreased left-sided hearing with recurrent ear infections indicative of possible CTCAE v4 grade 3 osteoradionecrosis of the

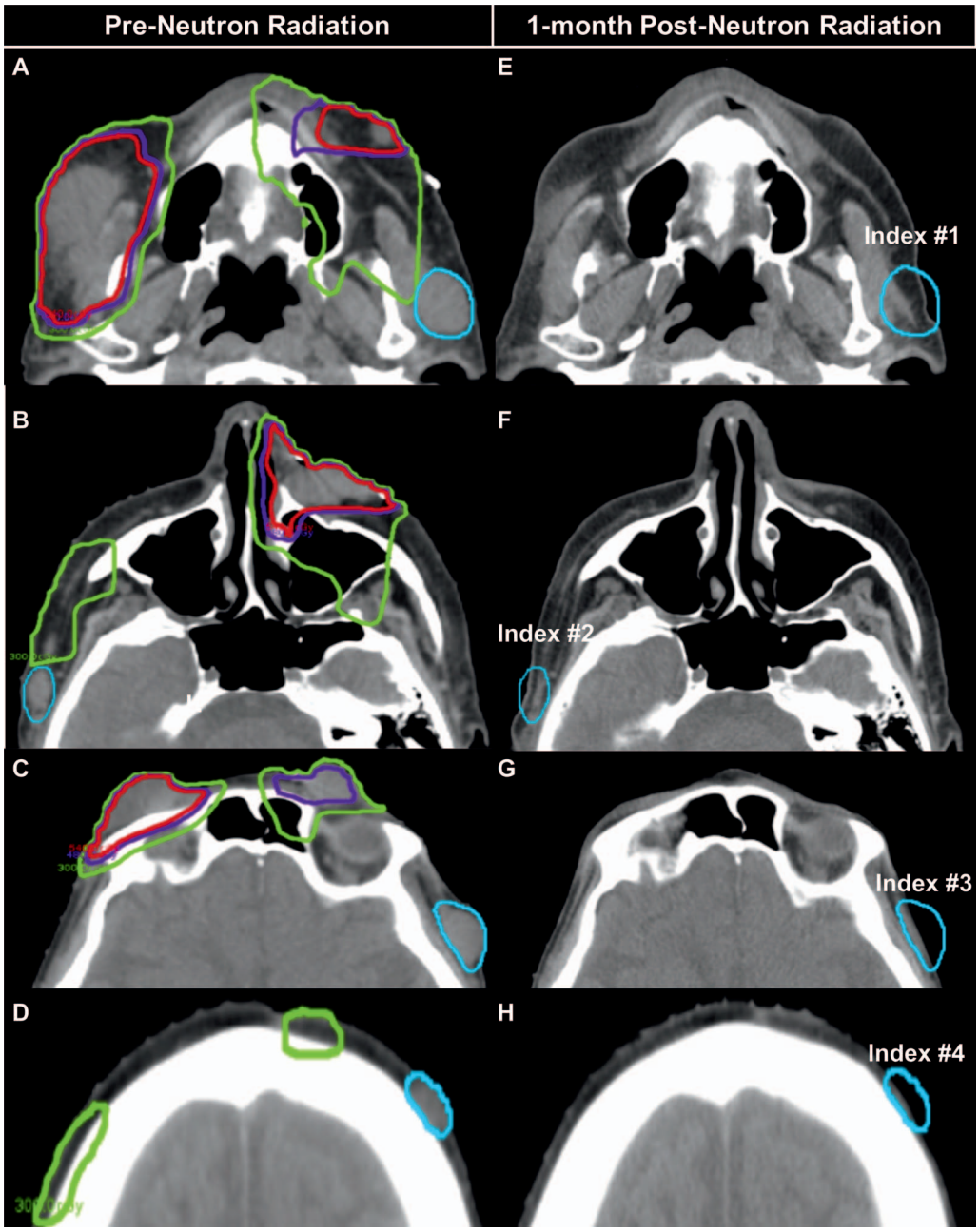

Figure 2. Patient A computed tomography scans before and after radiation treatment. Panels A through D show the 90% isodose line (IDL) (red), 80% IDL (purple), and 50% IDL (green) that represents the radiation field edge, with respect to the out-of-field lesions (blue). Panels E through H: The out-of-field lesions (blue) exhibit a complete response.

temporal bone. These toxicities were in the sites of re-irradiation, which were at an elevated risk due to the higher cumulative dose.

Comparative Assessment of Patient A and B Dosimetry

Details of the models and methods used to compute neutron RBE and XRT-equivalent EQD2 values are described in the **Appendix**. **Table 2** compares the equivalent NRT and XRT tumor doses for patients A and B to selected XRT treatments from the literature and to a conventional NRT treatment (1.15 Gy per day). All of the NRT and XRT in-field and out-of-field tumor doses in **Table 2** are for $(\alpha/\beta) = 3$ Gy. For comparison to the **Table 1** OAR plan constraints, **Table 3** summarizes mean OAR doses for the treatment of patient A with NRT.

Prior to NRT, patient B received a total EQD2 of 73.6 Gy to the entire scalp: 91.2 Gy to the frontal scalp and 52 Gy to the left neck and parotid. The NRT treatments in July 2015 correspond to a photon EQD2 of 99.5 Gy (16 Gy in 8 fractions) to the frontal scalp, 106.7 Gy (18 Gy in 10 fractions) to the parotid/cervical nodes, and 98.8 Gy (18 Gy in 12 fractions) to the central

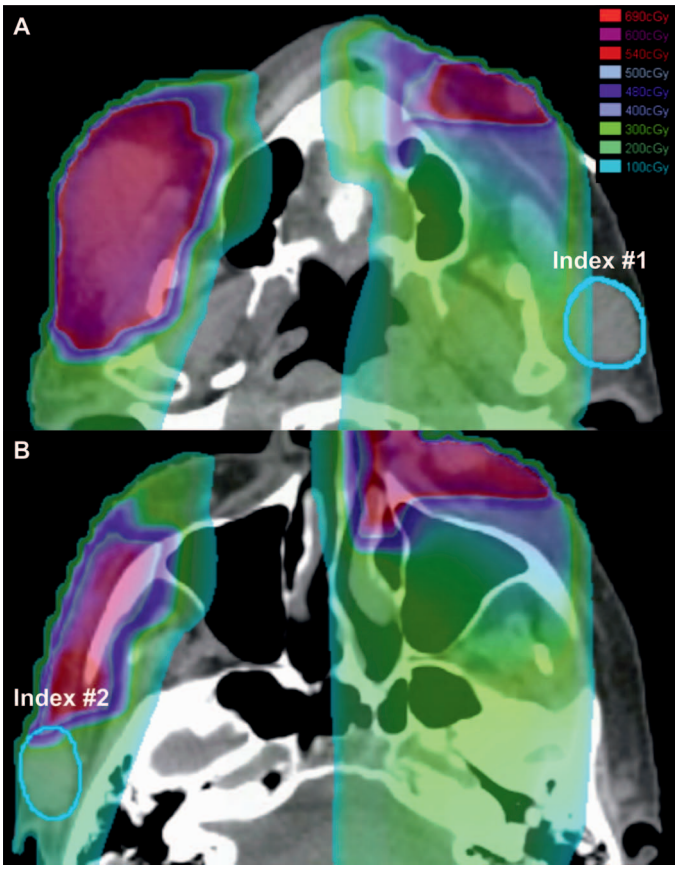

Figure 3. Patient A's neutron radiation therapy (NRT) 2 × 3 Gy plan showing radiation dose clouds (range: 1 to 6.9 neutron-Gy) demonstrating the out-of-field index lesions (blue) that were at the NRT field edge (A: index No. 1 1.0 neutron-Gy; B: index No. 2 1.98 neutron-Gy).

scalp. From the comparison of XRT and NRT EQD2 values, one might assume that NRT may exhibit slightly superior local control because of the larger effective dose, that is, EQD2 values in range from 73.6 (entire scalp) to 91.2 Gy (frontal scalp) XRT compared with 98.5 Gy to 106.7 Gy NRT. However, clinical observations indicate that the main difference between the XRT and NRT treatments is that patient B had a rapid, complete and *durable* response to NRT whereas the disease rapidly recurred and progressed when treated with XRT or immunotherapy. Although patient B subsequently enrolled in several immunotherapy trials after small volume out-of-field recurrences, he remained disease free after restarting anti-PD1 systematic therapy with pembrolizumab, which was previously ineffective. It is tempting to speculate that the NRT and/or subsequent immunotherapy may have helped initiate a durable antitumor immune response; however, direct laboratory evidence of antitumor immune activity is currently lacking.

Useful insights into the clinical significance of shorter and longer courses of NRT can be gained by comparing the NRT dosimetry for patients A and B. The EQD2 for Patient B (∼100 Gy) is over a factor of 2 larger than the EQD2 for patient A (∼46 Gy)[1]. However, the treated lesions in patients A and B had a rapid and complete clinical response. These observations suggest that a short course of NRT may be an effective treatment option for patients with recurrent lesions that are refractory to low LET radiations. Additional follow-up of Patient A is needed to confirm that the in-field response to a short course of NRT is as durable as a higher dose NRT treatment.

As expected, the EQD2 for the out-of-field lesions in patient A are much lower than the in-field dosimetry in the same patient. One out-of-field lesion received a 5-fold lower EQD2 of 9.4 Gy, whereas the other 3 out-of-field lesions received an EQD2 10-fold to 42-fold lower than the treated lesions (EQD2 of 1 to 4 Gy compared with 46 Gy for the treated lesions). As another point of reference, it is interesting to note that all of the out-of-field lesions received an EQD2 from the NRT almost a factor of 2 smaller than the EQD2 of 17.6 Gy, which corresponds to 1 × 8 Gy of XRT. These observations can either be taken as strong evidence for an out-of-field potentiation of antitumor activity or as evidence that patients with recurrent disease

[1] The 2-fold difference in EQD2 values for patients A and B is relatively insensitive to the tumor α/β. For $\alpha/\beta = 10$ Gy instead of 3 Gy (as in **Table 2**), the EQD2 for patient B is 70 Gy, and the EQD2 for patient A is 28.6 Gy. The ratio of the EQD2 for patient B divided by the EQD2 for patient A is 2.4 with $\alpha/\beta = 10$ Gy instead of 2 for $\alpha/\beta = 3$ Gy.

Table 2. Comparison of Merkel cell carcinoma lesion dosimetry for patients A and B.[a]

	NRT dose (Gy)				Equivalent XRT dose[c] (Gy)		
Patient[b]	n	Total	Fraction size	RBE[c]	Total	Fraction Size	EQD2
In-field dosimetry							
*	1	2.52	2.52	3.2	8.00	8.00	17.6
*	1	10.58	10.58	2.8	30.00	30.00	198.0
A	2	6.00	3.00	3.1	18.67	9.34	46.1
*	3	7.57	2.52	3.2	24.00	8.00	52.8
B	8	16.00	2.00	3.3	52.22	6.53	99.5
B	10	18.00	1.80	3.3	59.56	5.96	106.7
*	10	8.04	0.80	3.7	30.00	3.00	36.0
B	12	18.00	1.50	3.4	61.07	5.09	98.8
*	16	18.40	1.15	3.5	64.91	4.06	91.6
Out-of-field dosimetry							
A	2	0.32	0.16	4.7	1.51	0.75	1.1
A	2	0.44	0.22	4.5	1.99	1.00	1.6
A	2	1.00	0.50	4.0	4.02	2.01	4.0
A	2	1.98	0.99	3.6	7.15	3.57	9.4

Abbreviations: NRT, neutron radiation therapy; RBE, relative biological effectiveness; XRT, x-ray radiation therapy; EQD2, equivalent dose at 2 Gy.

[a]Patient A was treated with 2×3 neutron-Gy (in-field), and patient B was treated with 8 to 12 fractions for a total of 16 to 18 Gy.

[b]To provide additional clinical context, equivalent XRT and NRT doses are also listed for alternative treatment schedules (Patient *).

[c]Estimates of neutron RBE and equivalent XRT dose are for $(\alpha/\beta) = 3$ Gy.

refractory to low LET radiations and immunotherapy can achieve a complete clinical response with doses as low as 0.3 to 2 Gy NRT (EQD2 of 1.1 to 9.4 Gy). The former hypothesis seems more likely than the latter hypothesis given published studies [22, 23], and our experience with the treatment of MCC resistant to XRT.

The mean and maximum NRT dose, as well as the equivalent XRT dose for selected OARs of concern in the treatment of patient A are listed in **Table 3**. For the cornea, estimates of neutron RBE and EQD2 are based on $(\alpha/\beta) = 1$. For other OARs, the value of (α/β) corresponds to the value used to estimate the corresponding neutron plan constraints listed in **Table 1**. In general, the use of a low rather than high value for (α/β) increases the neutron RBE and the equivalent EQD2 value for XRT. When used as a plan constraint, a low value of (α/β) for an OAR reduces the risk of treatment complications (ie, the plan constraint is more dose limiting for tumor targets). The use of lower values of (α/β) also tends to overestimate the risks of treatment complications when comparing patient-specific OAR dosimetry (**Table 3**) to a priori plan constraints (**Table 1**). For MCC patients with skin and subcutaneous lesions on their face treated with a short (2×3 Gy) course of NRT, the comparison of patient dosimetry and plan constraints suggests that OAR toxicity is unlikely for the lacrimal glands and critical structures in the eye. The doses to other OARs are also unlikely to exceed plan constraints. For example, a maximum OAR dose of 2×3 Gy NRT corresponds to an EQD2 for XRT of <56.5 Gy for the brain and brainstem, ≤ 39.5 Gy for the ears, and ≤ 28.6 Gy for

Table 3. Equivalent XRT and NRT dosimetry for selected OARs for Patient A (n = 2 fractions).

	NRT Dose (Gy)		RBE			XRT EQD2 (Gy)	
OAR	Mean	Maximum	Mean	Maximum	α/β (Gy)	Mean	Maximum
Right optic nerve	0.48	0.56	4.7	4.6	2.4	1.8	2.2
Left optic nerve	0.58	0.99	4.6	4.2	2.4	2.2	4.2
Optic chiasm	0.55	0.94	4.6	4.2	2.4	2.1	3.9
Right lens	1.09	1.98	4.4	3.8	1.0	5.5	12.1
Left lens	1.01	1.24	4.5	4.3	1.0	5.0	6.5
Right cornea	1.29	2.73	3.8	3.6	1.0	6.8	19.2
Left cornea	2.01	3.54	3.5	3.4	1.0	12.4	28.3
Right lacrimal gland	1.00	2.10	4.6	3.8	0.9	5.0	13.4
Left lacrimal gland	0.58	0.61	5.3	5.2	0.9	2.6	2.7

Abbreviations: XRT, x-ray radiation therapy; NRT, neutron radiation therapy, OAR, organ at risk; RBE, relative biological effectiveness; EQD2, equivalent dose at 2 Gy,

the skin. The plan constraints in **Table 1** are based on historical University of Washington clinical experience with NRT in patients who did not receive concurrent immunotherapy, and the plan constraints listed in **Table 1** should be used with caution because of the unknown potential for elevated risks from combining NRT and checkpoint blockade systemic therapy.

Discussion and Conclusions

To our knowledge, this is the first case series in the literature describing NRT for the treatment of MCC refractory to low LET radiation. The rapid tumor response to NRT allowed functional preservation of patient A's eyes with negligible toxicity, in addition to producing an out-of-field abscopal response that is likely immune mediated. It remains to be seen whether high LET radiations are more effective at potentiating an immune response than low LET radiations.

The concept of radiation therapy as a vaccine to instigate tumor antigen release and consequently promote an enhanced antitumor immune response is a relatively new area of active investigation. The vast majority of the work published to date is based on low LET radiation therapy (eg, electrons, megavoltage x-rays, and protons) because of the widespread availability of treatment facilities. Clinical reports have shown that low LET radiation therapy directed toward one tumor can occasionally result in an abscopal (off-target) effect in patients exhibiting progression on immunotherapy [17, 24]. Additionally, preclinical and clinical data suggest that low LET radiation therapy can work in synergy with immune checkpoint blockade to trigger an abscopal response in a wide variety of tumor types [24–28]. A case of an abscopal effect without immunotherapy was recently described with carbon ions after a full course of treatment that is generally associated with significant toxicity [29, 30]. The role of high LET radiation and immunotherapy was recently reviewed in detail elsewhere [30, 31]. Patient A represents the first report to demonstrate an off-target/out-of-field response using a short course of NRT in combination with checkpoint blockade immunotherapy. The idea of trying to elicit an abscopal response was based on the work of Postow et al [17], who demonstrated an abscopal response in melanoma with the use of an XRT prescription of 3×9.5 Gy delivered within 7 days. The neutron RT dose-fractionation scheme of 2×3 Gy delivered weekly was derived using an RBE conversion factor of approximately 3 for NRT. Minimal toxicity with durable disease control was observed in the patient after nine months of follow-up, while he continued on an immune checkpoint inhibitor. While the details of the underlying mechanisms remain to be elucidated, there appears to be a strong role for CD8+ effector T-cells, cytokine release, and a decrease in myeloid-derived suppressor cells [17, 24, 25].

A 1×8 Gy treatment of low-LET radiation (multivoltage x-rays or electrons) was selected initially for patient A in the postoperative setting over standard-of-care conventional fractionated radiation therapy (46-50 Gy in 4.5-5 weeks) due to the patient's medical comorbidities, and logistical problems with attending a protracted course of radiation therapy. Use of 1×8 Gy with low LET XRT (EQD2 = 17.6 Gy) was based on our group's prior experience with this regimen among patients with metastatic disease, which was associated with a local control rate of 77% [32]. In patient A, 1×8 Gy of low LET radiation sufficed to prevent an in-field local regional recurrence at sites of potential microscopic disease in the resected glabellar primary (positive margin) and sentinel node positive neck level-2 region. However, it failed to provide durable local control for the recurrent macroscopic disease sites, and it is unclear what, if any, role his immune status may have played in the process. These observations are in keeping with our published experience correlating higher rates of in-field progression in immunosuppressed patients [32] and preclinical studies showing impaired tumoricidal effects of radiation therapy in immunodeficient mice [33]. A review of 812 patients by Tseng et al [34] of stage I to III MCC treated with conventional XRT similarly showed that immunosuppressed MCC patients have decreased local control and inferior relapse-free survival compared with immune competent patients. That is, they are more radiation resistant.

The poor durability of response to XRT in patients A and B motivated the use of NRT with palliative intent. One of the potential reasons NRT may have a greater capacity for potentiating the immune response is that the modes and kinetics of reproductive cell death differ for low and high LET radiations [35, 36]. A number of in vitro studies have found that apoptosis is initiated by high LET radiation independent of p53 status, whereas low LET radiations are less effective at initiating apoptosis in cells with a mutated or null p53 status [37–39]. Irradiation of p53-null cancer cells by high LET carbon ions favors mitotic catastrophe over apoptosis [40]. This could be relevant in MCC that arise from MCPyV infection in which the viral large T antigen has been shown to inactivate p53 and Rb [41].

Another challenge is identifying the optimal timing of radiation therapy and immunotherapy to potentiate an immune response. Patient A experienced clinical progression on immune checkpoint blockade therapy, and his progressive and painful tumors were threatening his vision. These observations prompted urgent consideration of radiation therapy for symptomatic lesions. Patient A continued on systemic immunotherapy while undergoing NRT. In comparison, patient B's anti-PD1 therapy

was discontinued 3 months before NRT. Patient B was only restarted on immunotherapy after out-of-field progression of disease 6 months later, and he exhibited a robust response to the same after initial progression through octreotide therapy. Patient B's palliative NRT course contributed toward his ability to enroll in subsequent systemic immunotherapy trials that eventually led to a durable complete response.

Young and colleagues [42] showed in murine models of colorectal cancer that anti-CTLA4 immunotherapy or radiation therapy (20 Gy in 1 fraction) alone had little effect on tumor control; however, CTLA4 administration 7 days before radiation therapy resulted in a complete response; conversely, only half responded to CTLA4 when administered 5 days after radiation therapy. Moreover, the mice that demonstrated a complete response were resistant when rechallenged with the same tumor, which is suggestive of a persistent or long-term immunity. Using the same murine model system, Dovedi et al [43] demonstrated that radiation therapy (10 Gy in 5 daily fractions) led to tumor PD-L1 expression upregulation at a peak of 3 days after radiation therapy, which declined significantly 7 days later. This corresponded to improved local control with combined radiation therapy and PD-L1/PD-1 axis blockade when checkpoint inhibition was administered on day 1 or day 5; conversely, at 7 days after completion of radiation therapy, when the PD-L1 expression had declined, addition of checkpoint blockade did not improve local control over radiation therapy alone. These observations support the importance of addressing the timing of immunotherapy administration and radiation treatments. However, this preclinical data contrast with clinical trials of checkpoint blockade in MCC, which have yet to show that tumor PD-L1 expression correlates with a higher response rate to immunotherapy [3].

The use of concurrent checkpoint blockade systemic therapy with NRT may stimulate an anti-immune response more than from NRT alone. In regard to low LET radiation, Luke et al [44] demonstrated in 73 patients with stage IV metastatic solid tumor the safety and clinical activity in a phase 1 trial of pembrolizumab administered within 7 days of multisite stereotactic body radiation therapy (1 to 4 treated sites). Targets exceeding $>$65 mL received only partial volume irradiation, where an exploratory subgroup analysis showed similar tumor control compared with total tumor irradiation, which is suggestive of a response in close vicinity to the radiation target by the combination of radiation and immunotherapy. However, the overall objective response rates remained low at 13.2%, further highlighting the need for additional studies to identify the optimal combination of radiation and immunotherapy for maximal efficacy.

Determining the impact of using hypofractionated stereotactic body radiation therapy in combination with immunotherapy in patients with advanced or metastatic MCC is the subject of an upcoming randomized phase 2 clinical trial (NCT03304639). Patients A and B receiving NRT suggests the importance of prospective evaluation of high LET radiation therapy as a promising alternative modality for potentiating an immune response. Although caution with combined NRT and immunotherapy is prudent, the cases discussed here provide evidence that low doses of NRT in combination with checkpoint blockade immunotherapy may be well tolerated. Systematic clinical trials are urgently needed to address key factors and challenges related to the individualization of treatment parameters with the goal of maximizing the response rate to radiation and immunotherapy.

ADDITIONAL INFORMATION AND DECLARATIONS

Conflicts of Interest Statement: The authors have no conflicts to disclose.

References

1. Miller NJ, Bhatia S, Parvathaneni U, Iyer JG, Nghiem P. Emerging and mechanism-based therapies for recurrent or metastatic Merkel cell carcinoma. *Curr Treat Options Oncol*. 2013;14:249–63.
2. Iyer JG, Blom A, Doumani R, Lewis C, Tarabadkar ES, Anderson A, Ma C, Bestick A, Parvathaneni U, Bhatia S, Nghiem P. Response rates and durability of chemotherapy among 62 patients with metastatic Merkel cell carcinoma. *Cancer Med*. 2016;5:2294–301.
3. Nghiem PT, Bhatia S, Lipson EJ, Kudchadkar RR, Miller NJ, Annamalai L, Berry S, Chartash EK, Daud A, Fling SP, Friedlander PA, Kluger HM, Kohrt HE, Lundgren L, Margolin K, Mitchell A, Olencki T, Pardoll DM, Reddy SA, Shantha EM, Sharfman WH, Sharon E, Shemanski LR, Shinohara MM, Sunshine JC, Taube JM, Thompson JA, Townson SM, Yearley JH, Topalian SL, Cheever MA. PD-1 Blockade with pembrolizumab in advanced Merkel-cell carcinoma. *N Engl J Med*. 2016;374:2542–52.

4. Laramore GE, Krall JM, Griffin TW, Duncan W, Richter MP, Saroja KR, Maor MH, Davis LW. Neutron versus photon irradiation for unresectable salivary gland tumors: final report of an RTOG-MRC randomized clinical trial. Radiation Therapy Oncology Group. Medical Research Council. *Int J Radiat Oncol Biol Phys*. 1993;27:235–40.
5. Sur RK, Donde B, Levin V, Pacella J, Kotzen J, Cooper K, Hale M. Adenoid cystic carcinoma of the salivary glands: a review of 10 years. Laryngoscope. 1997;107:1276–80.
6. Stewart RD, Yu VK, Georgakilas AG, Koumenis C, Park JH, Carlson DJ. Effects of radiation quality and oxygen on clustered DNA lesions and cell death. Radiat Res. 2011;176:587–602.
7. Bird RP, Burki HJ. Survival of synchronized Chinese hamster cells exposed to radiation of different linear-energy transfer. *Int J Radiat Biol Relat Stud Phys Chem Med*. 1975;27:105–20.
8. Blakely EA, Chang PY, Lommel L. Cell-cycle-dependent recovery from heavy-ion damage in G1-phase cells. *Radiat Res Suppl*. 1985;8:S145–57.
9. Ngo FQ, Blakely EA, Tobias CA, Chang PY, Lommel L. Sequential exposures of mammalian cells to low- and high-LET radiations. II. As a function of cell-cycle stages. *Radiat Res*. 1988;115:54–69.
10. Schlaich F, Brons S, Haberer T, Debus J, Combs SE, Weber KJ. Comparison of the effects of photon versus carbon ion irradiation when combined with chemotherapy in vitro. *Radiat Oncol*. 2013;8:260.
11. Barendsen GW, Van Bree C, Franken NA. Importance of cell proliferative state and potentially lethal damage repair on radiation effectiveness: implications for combined tumor treatments (review). *Int J Oncol*. 2001;19:247–56.
12. Asaithamby A, Uematsu N, Chatterjee A, Story MD, Burma S, Chen DJ. Repair of HZE-particle-induced DNA double-strand breaks in normal human fibroblasts. *Radiat Res*. 2008;169:437–46.
13. Antonelli F, Campa A, Esposito G, Giardullo P, Belli M, Dini V, Meschini S, Simone G, Sorrentino E, Gerardi S, Cirrone GA, Tabocchini MA. Induction and repair of DNA DSB as revealed by H2AX phosphorylation foci in human fibroblasts exposed to low- and high-LET radiation: relationship with early and delayed reproductive cell death. *Radiat Res*. 2015; 183:417–31.
14. Rubner Y, Wunderlich R, Rühle PF, Kulzer L, Werthmöller N, Frey B, Weiss EM, Keilholz L, Fietkau R, Gaipl US. How does ionizing irradiation contribute to the induction of anti-tumor immunity? *Front Oncol*. 2012;2:75.
15. Meng MB, Wang HH, Cui YL, Wu ZQ, Shi YY, Zaorsky NG, Deng L, Yuan ZY, Lu Y, Wang P. Necroptosis in tumorigenesis, activation of anti-tumor immunity, and cancer therapy. *Oncotarget*. 2016;7:57391–413.
16. Wu Q, Allouch A, Martins I, Brenner C, Modjtahedi N, Deutsch E, Perfettini JL. Modulating both tumor cell death and innate immunity is essential for improving radiation therapy effectiveness. *Front Immunol*. 2017;8:613.
17. Postow MA, Callahan MK, Barker CA, Yamada Y, Yuan J, Kitano S, Mu, Z, Rasalan T, Adamow M, Ritter E, Sedrak C, Jungbluth AA, Chua R, Yuang AS, Roman R, Rosner S, Benson B, Allison JP, Lesokhin AM, Gnjatic S, Wolchok JD. Immunologic correlates of the abscopal effect in a patient with melanoma. *N Engl J Med*. 2012;366:925–31.
18. Macomber MW, Tarabadkar ES, Mayr NA, Laramore GE, Bhatia S, Tseng YD, Liao J, Arbuckle T, Ngheim P, Parvathaneni U. Neutron radiation therapy for treatment of refractory Merkel cell carcinoma. *Int J Part Ther*. 2017;3:485–91.
19. Gunderson LL, Tepper JE. *Clinical Radiation Oncology*. 4th ed. Philadelphia, PA: Elsevier Saunders; 2012.
20. Battermann JJ, Breur K, Hart GA, van Peperzeel HA. Observations on pulmonary metastases in patients after single doses and multiple fractions of fast neutrons and cobalt-60 gamma rays. *Eur J Cancer*. 1981;17:539–48.
21. Kalet AM, Sandison GA, Phillips MH, Parvathaneni U. Validation of the Pinnacle(3) photon convolution-superposition algorithm applied to fast neutron beams. *J Appl Clin Med Phys*. 2013;14:4305.
22. Cimbak N, Barker CA Jr. Short-course radiation therapy for Merkel cell carcinoma: relative effectiveness in a "radiosensitive" tumor. *Int J Radiat Oncol Biol Phys*. 2016;96:S160.
23. Filatenkov A, Baker J, Mueller AM, Kenkel J, Ahn GO, Dutt S, Zhang N, Kohrt H, Jensen K, Dejbakhsh-Jones S, Shizuru JA, Negrin RN, Engleman EG, Strober S. Ablative tumor radiation can change the tumor immune cell microenvironment to induce durable complete remissions. *Clin Cancer Res*. 2015;21:3727–39.
24. Twyman-Saint Victor C, Rech AJ, Maity A, Rengan R, Pauken KE, Stelekati E, Benci JL, Xu B, Dada H, Odorizzi PM, Herati RS, Mansfield KD, Patsch D, Amaravadi RK, Schuchter LM, Ishwaran H, Mick R, Pryma D. Radiation and dual checkpoint blockade activate non-redundant immune mechanisms in cancer. *Nature*. 2015;520:373–7.

25. Demaria S, Kawashima N, Yang AM, Devitt ML, Babb JS, Allison JP, Formenti SC. Immune-mediated inhibition of metastases after treatment with local radiation and CTLA-4 blockade in a mouse model of breast cancer. Clin Cancer Res. 2005;11:728–34.
26. Dewan MZ, Galloway AE, Kawashima N, Dewyngaert JK, Babb JS, Formenti SC, Demaria S. Fractionated but not single-dose radiotherapy induces an immune-mediated abscopal effect when combined with anti-CTLA-4 antibody. *Clin Cancer Res*. 2009;15:5379–88.
27. Golden EB, Chhabra A, Chachoua A, Adams S, Donach M, Fenton-Kerimian M, Friedman K, Ponzo F, Babb JS, Goldberg J, Demaria S, Formenti SC. Local radiotherapy and granulocyte-macrophage colony-stimulating factor to generate abscopal responses in patients with metastatic solid tumours: a proof-of-principle trial. *Lancet Oncol*. 2015;16:795–803.
28. Golden EB, Demaria S, Schiff PB, Chachoua A, Formenti SC. An abscopal response to radiation and ipilimumab in a patient with metastatic non-small cell lung cancer. *Cancer Immunol Res*. 2013;1:365–72.
29. Ebner DK, Kamada T, Yamada S. Abscopal effect in recurrent colorectal cancer treated with carbon-ion radiation therapy: 2 case reports. *Adv Radiat Oncol*. 2017;2:333–8.
30. Durante M, Brenner DJ, Formenti SC. Does heavy ion therapy work through the immune system? *Int J Radiat Oncol Biol Phys*. 2016;96:934–6.
31. Shimokawa TM, L; Ando, K; Sato, K; Imai T. The future of combining carbon-ion radiotherapy with immunotherapy: evidence and progress in mouse models. *Int J Part Ther*. 2016;3:66–70.
32. Iyer JG, Parvathaneni U, Gooley T, Miller NJ, Markowitz E, Blom A, Lewis CW, Doumani RF, Parvathaneni K, Anderson A, Bestick A, Liao J, Kane G, Bhatia S, Paulson K, Nghiem P. Single-fraction radiation therapy in patients with metastatic Merkel cell carcinoma. *Cancer Med*. 2015;4:1161–70.
33. Lee Y, Auh SL, Wang Y, Burnette B, Wang Y, Meng Y, Beckett M, Sharma R, Chin R, Tu T, Weichselbaum RR, Fu YX. Therapeutic effects of ablative radiation on local tumor require CD8+ T cells: changing strategies for cancer treatment. *Blood*. 2009;114:589–95.
34. Tseng YD, Nguyen MH, Baker K, Cook M, Redman M, Lachance K, Bhatia S, Liao JJ, Apisarnthanarax S, Nghiem PT, Parvathaneni U. Effect of host immune status on the efficacy of radiotherapy and recurrence-free survival among 812 Merkel cell carcinoma patients. *Int J Rad Onc Bio Phys*. 2018. In press.
35. Maalouf M, Alphonse G, Colliaux A, Beuve M, Trajkovic-Bodennec S, Battiston-Montagne P, Testard I, Chapet O, Bajard M, Taucher-Scholz G, Fournier C, Rodriguez-Lafrasse C. Different mechanisms of cell death in radiosensitive and radioresistant p53 mutated head and neck squamous cell carcinoma cell lines exposed to carbon ions and x-rays. *Int J Radiat Oncol Biol Phys*. 2009;74:200–9.
36. Kobayashi D, Oike T, Shibata A, Niimi A, Kubota Y, Sakai M, Amornwhichet N, Yoshimoto Y, Hagiwara Y, Kimura Y, Hirota Y, Sato H, Isono M, Yoshida Y, Kohno T, Ohno T, Nakano T. Mitotic catastrophe is a putative mechanism underlying the weak correlation between sensitivity to carbon ions and cisplatin. *Sci Rep*. 2017;7:40588.
37. Takahashi A, Matsumoto H, Yuki K, Yasumoto J, Kajiwara A, Aoki M, Furusawa Y, Ohnishi K, Ohnishi T. High-LET radiation enhanced apoptosis but not necrosis regardless of p53 status. *Int J Radiat Oncol Biol Phys*. 2004;60:591–7.
38. Takahashi A, Matsumoto H, Furusawa Y, Ohnishi K, Ishioka N, Ohnishi T. Apoptosis induced by high-LET radiations is not affected by cellular p53 gene status. *Int J Radiat Biol*. 2005;81:581–6.
39. Mori E, Takahashi A, Yamakawa N, Kirita T, Ohnishi T. High LET heavy ion radiation induces p53-independent apoptosis. *J Radiat Res*. 2009;50:37–42.
40. Amornwichet N, Oike T, Shibata A, Ogiwara H, Tsuchiya N, Yamauchi M, Saitoh Y, Sekine R, Isono M, Yoshida Y, Ohno T, Kohno T, Nakano T. Carbon-ion beam irradiation kills x-ray-resistant p53-null cancer cells by inducing mitotic catastrophe. *PLoS One*. 2014;9:e115121.
41. Feng H, Shuda M, Chang Y, Moore PS. Clonal integration of a polyomavirus in human Merkel cell carcinoma. *Science*. 2008;319:1096–100.
42. Young KH, Baird JR, Savage T, Cottam B, Friedman D, Bambina S, Messenheimer DJ, Fox B, Newell P, Bahjat KS, Gough MJ, Crittenden MR. Optimizing timing of immunotherapy improves control of tumors by hypofractionated radiation therapy. *PLoS One*. 2016;11:e0157164.

43. Dovedi SJ, Adlard AL, Lipowska-Bhalla G, McKenna C, Jones S, Cheadle EJ, Stratford IJ, Poon E, Morrow M, Stewart R, Jones H, Wilkinson RW, Honeychurch J, Illidge TM. Acquired resistance to fractionated radiotherapy can be overcome by concurrent PD-L1 blockade. *Cancer Res*. 2014;74:5458–68.
44. Luke JJ, Lemons JM, Karrison TG, Pitroda SP, Melotek JM, Zha Y, Al-Hallaq HA, Arina A, Khodarev NN, Janisch L, Chang P, Patel JD, Fleming GF, Moroney J, Sharma MR, White JR, Ratain MJ, Gajewski TF, Weichselbaum RR, Chmura SJ. Safety and clinical activity of fembrolizumab and multisite stereotactic body radiotherapy in patients with advanced solid tumors. *J Clin Oncol*. 2018;36:1611–8.
45. Carlson DJ, Stewart RD, Semenenko VA, Sandison GA. Combined use of Monte Carlo DNA damage simulations and deterministic repair models to examine putative mechanisms of cell killing. *Radiat Res*. 2008;169:447–59.
46. Frese MC, Yu VK, Stewart RD, Carlson DJ. A mechanism-based approach to predict the relative biological effectiveness of protons and carbon ions in radiation therapy. *Int J Radiat Oncol Biol Phys*. 2012;83:442–50.
47. International Commission on Radiation Units and Measurements, ICRU Report 36, Microdosimetry, Bethesda, Maryland, (1983).
48. Stewart RD, Streitmatter SW, Argento DC, Kirkby C, Goorley JT, Moffitt G, Jevremovic T, Sandison GA. Rapid MCNP simulation of DNA double strand break (DSB) relative biological effectiveness (RBE) for photons, neutrons, and light ions. *Phys Med Biol*. 2015;60:8249–74.

Appendix. Biological Metrics of Comparative NRT and XRT Treatment Effectiveness

As an aid in comparing megavoltage x-ray treatments to NRT treatments, we computed the biologically equivalent dose and equivalent dose in 2 Gy fractions using the Repair-Misrepair-Fixation (RMF) model [45, 46] to correct for neutron relative biological effectiveness (RBE). In the linear-quadratic approximation to the RMF model, neutron RBE for fraction size d can be written as

$$RBE(d) = \frac{(\alpha/\beta)}{2d}\left\{-1+\sqrt{1+\frac{4d}{(\alpha/\beta)}\left(1+\frac{d}{(\alpha/\beta)}\frac{(RBE_{HD})^2}{RBE_{LD}}\right)}\,RBE_{LD}\right\}. \tag{A1}$$

Here, $\overline{z}_F$ is the frequency-mean specific energy (ICRU 1983) [47]; the low dose RBE for cell survival (RBE_{LD}) is

$$RBE_{LD} = RBE_{DSB}\left(1+\frac{2\overline{z}_F RBE_{DSB}}{(\alpha/\beta)}\right) \geq RBE_{DSB}, \tag{A2}$$

and the high dose RBE (RBE_{HD}), that is, the RBE in the limit as the fraction size becomes large compare to (α/β), is

$$RBE_{HD} = RBE_{DSB} \geq 1. \tag{A3}$$

For a spherical target of diameter d_N and density ρ, $\overline{z}_F \cong LET/\rho d_N^2 = 0.58$Gy for Clinical Neutron Therapy System (CNTS) neutrons (linear energy transfer [LET] ~60.6 keV/μm) and d_N 4.6 μm. In equations (A2) and (A3), the independently tested Monte Carlo Damage Simulation (MCDS) to estimate the RBE_{DSB} [RBE for DNA double-strand break (DSB) induction] from first principles, For CNTS fast neutrons, $RBE_{DSB} \cong 2.7 + 0.1$ [48]. Although DSBs are widely considered one of the most biologically critical forms of DNA damage, the vast majority of initial DSBs formed by low and high LET ionizing radiation (>98%) are correctly rejoined. In the RMF model, RBE_{HD} approaches RBE_{DSB} because the chromosome aberrations (mainly exchanges) formed by the incorrect rejoining of break ends by low and high LET radiations are equally lethal. The main difference between the incorrect rejoining of DSBs formed by low and high LET radiations is the kinetics of the repair process, which is implicitly reflected in the tumor-specific and tissue-specific value of (α/β).

Because the independently tested MCDS is used to estimate RBE_{DSB} from first principles [6, 48], the conversion of an NRT dose into an equivalent XRT dose is uniquely determined by the particle-specific and tissue-specific product of $\overline{z}_F/(\alpha/\beta) \cong LET/(\alpha/\beta)d_N^2$ where d_N is the effective diameter of the cell nucleus. As a first approximation, it is reasonable to assume that the effective LET and diameter of the cell nucleus are approximately the same for all irradiated tissue within the human body. Neutron RBE varies among tissues and tumor cells because of the value of (α/β). For CNTS-generated fast neutrons, the majority of the absorbed dose at the cellular-level arises from secondary charged particles, mainly low energy $^1H^+$ and $^4He^{2+}$ ions. An effective LET of 60.6 keV/μm and $d_N = 4.6$ μm ($\overline{z}_F = 0.58$ Gy) gives neutron RBE values consistent with University of Washington clinical experience. For CNTS neutrons and (α/β) = 10 Gy, $RBE_{LD} = 3.54$ and $RBE_{HD} = 2.7$. As indicated by

equation (A2), the value of RBE_{LD} increases with decreasing (α/β). For example, RBE_{LD} increases to 11.1 for an (α/β) = 1 Gy. For any fraction size d, the value of RBE(d) computed using equation (A1) will fall within the range (RBE_{HD}, RBE_{LD}). After computing the tumor-specific and tissue-specific value for RBE(d) using equations (A1) to (A3), the photon-equivalent biologically equivalent dose (in Gy) for an n-fraction treatment is computed as

$$BED(D,d) = D \cdot RBE(d)\left(1 + \frac{d \cdot RBE(d)}{\alpha/\beta}\right), \text{ where } D \equiv nd. \tag{A4}$$

The photon-equivalent EQD2 (in Gy) is computed as

$$EQD2 = \frac{BED(D,d)}{\left(1 + \frac{2\text{Gy}}{\alpha/\beta}\right)} = \frac{\left(1 + \frac{d \cdot RBE(d)}{\alpha/\beta}\right)}{\left(1 + \frac{2\text{Gy}}{\alpha/\beta}\right)} D. \tag{A5}$$

It is important to note that, in equations (A1) and (A5), the value of (α/β) is for the reference radiation (ie, megavoltage x-rays) rather than fast neutrons.